SUPPORTING INFORMATION

B–H Bond Activation using an Electrophilic Metal Complex: Insights into the Reaction Pathway

*Rahul Kumar and Balaji R. Jagirdar**

Department of Inorganic & Physical Chemistry, Indian Institute of Science, Bangalore 560012, India

CONTENTS

(b) ^{31}P NMR spectral stack plot showing the P_{ax} and P_{eq} signals getting broadened and resharpen with downfield shift at low temperature

Figure S22. Variable temperature NMR spectral stack plots for complex **1** (BLANK) in CD_2Cl_2: (a) $^{31}P\{^1H\}$ NMR spectral stack plot showing the P_{ax} and P_{eq} signals getting broadened and resharpen with downfield shift at low temperature; (b)^{19}F NMR spectral stack plot showing a singlet for triflate (OTf) counter ion which broadened at 223 K and shifts upfield

Figure S23. $^{31}P\{^1H\}$ Inversion recovery spectral stack plot for the reaction of complex **1** with DMAB in CD_2Cl_2 with mixing time delay (τ_{mix}) at room temperature showing change in intensity of **4** when **6** is inverted selectively and recovered with τ_{mix}

Figure S24. Spin-saturation transfer experiment: ^1H NMR (upfield region) spectral stack plots for the reaction of complex **1** with DMAB in CD_2Cl_2 at room temperature; (a) irradiation of **5**, (b) irradiation of **6**

Figure S25. $^{31}P\{^1H\}$ Spin-saturation transfer spectral stack plot for the reaction of complex **1** with DMAB in CD_2Cl_2 at room temperature,* = *trans*-[$RuCl_2(dppe)_2$]

Figure S26. $^{31}P\{^1H\}$ Spin-saturation transfer spectral stack plot for the reaction of complex **1** with DMAB in CD_2Cl_2 at room temperature after irradiation of **4**, * = *trans*-[$RuCl_2(dppe)_2$] (Note: spectra in Figures S25 and S26 are from different batches)

Figure S27. $^{31}P\{^1H\}$ Inversion recovery spectral stack plot for the reaction of complex **1** with DMAB in CD_2Cl_2 with mixing time delay (τ_{mix}) at 203 K showing change in intensity of **4** when **7** is inverted selectively and recovered with τ_{mix}, * = **3b** is also getting affected. **Note**: only the peaks getting affected after inversion of **7** and during its recovery are shown

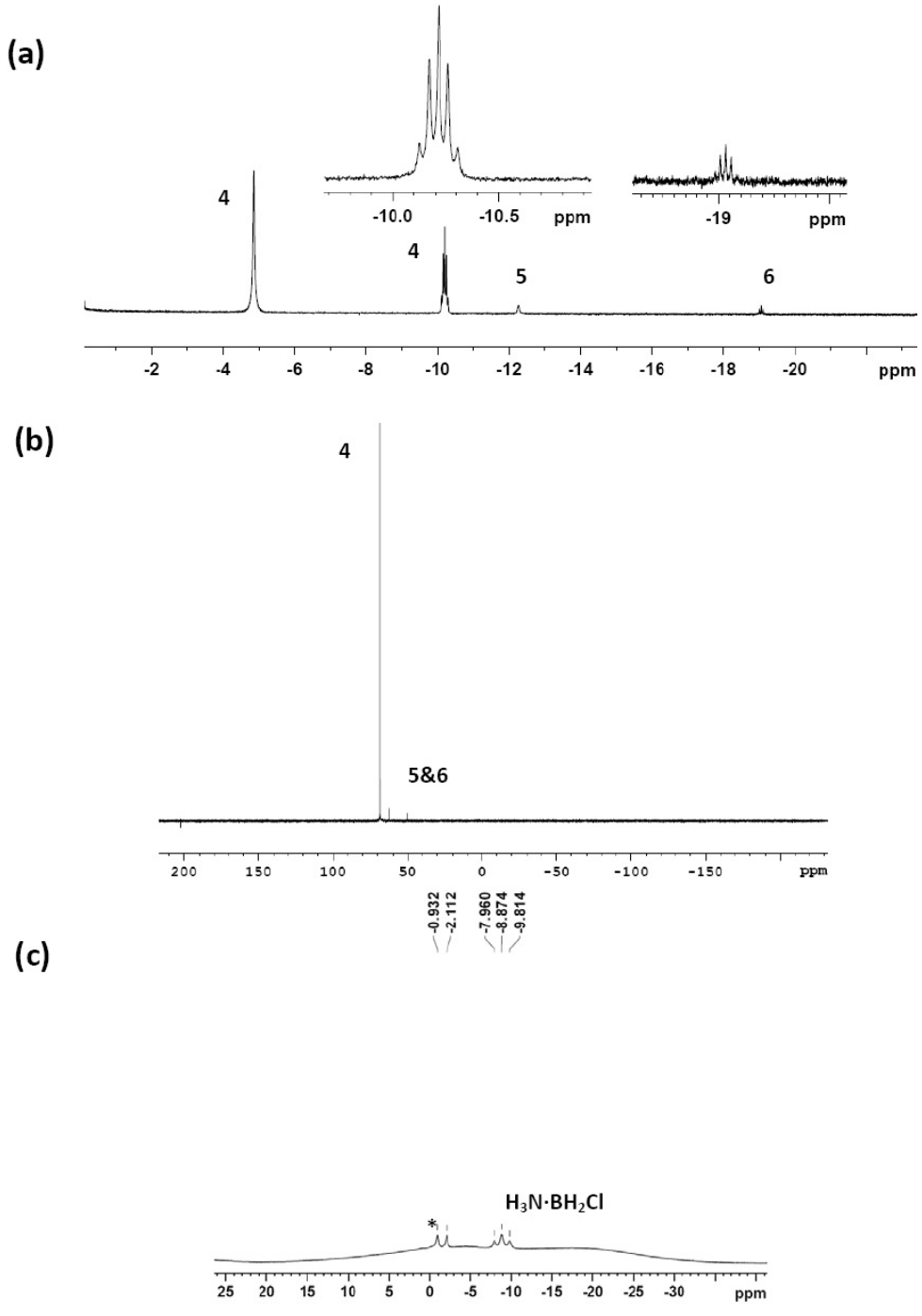

Figure S1. (a) ^{1}H, (b) $^{31}P\{^{1}H\}$, (c) ^{11}B NMR spectra of the reaction of complex **1** with AB (1:1) at room temperature

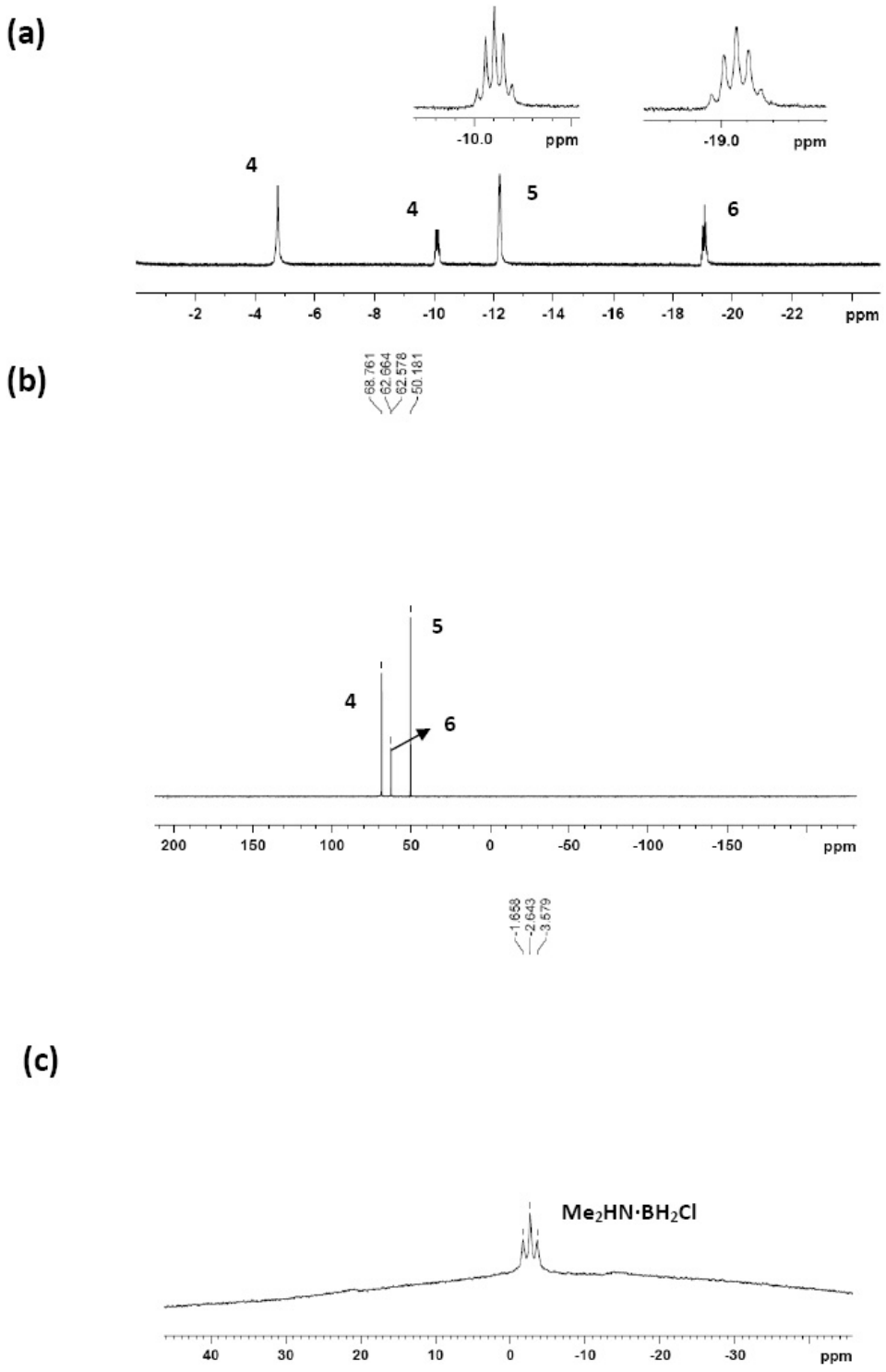

Figure S2. (a) ^{1}H, (b) $^{31}P\{^{1}H\}$, (c) ^{11}B NMR spectra of the reaction of complex **1** with DMAB (1:1) at room temperature

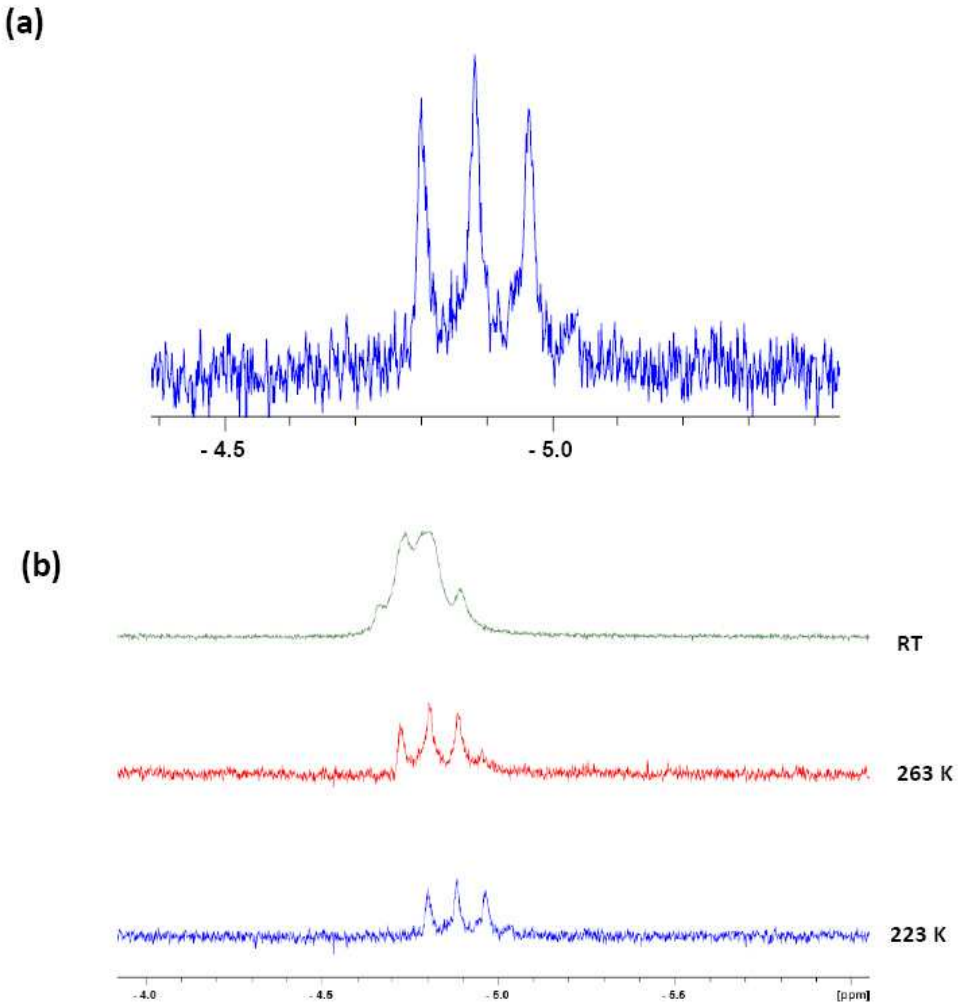

Figure S3. (a) ^{1}H NMR spectrum of the reaction of complex **1** with $H_3N{\cdot}BD_3$ (ABD) at 253 K, (b) VT ^{1}H NMR spectral stack plot showing evolution of mixed isotopomers

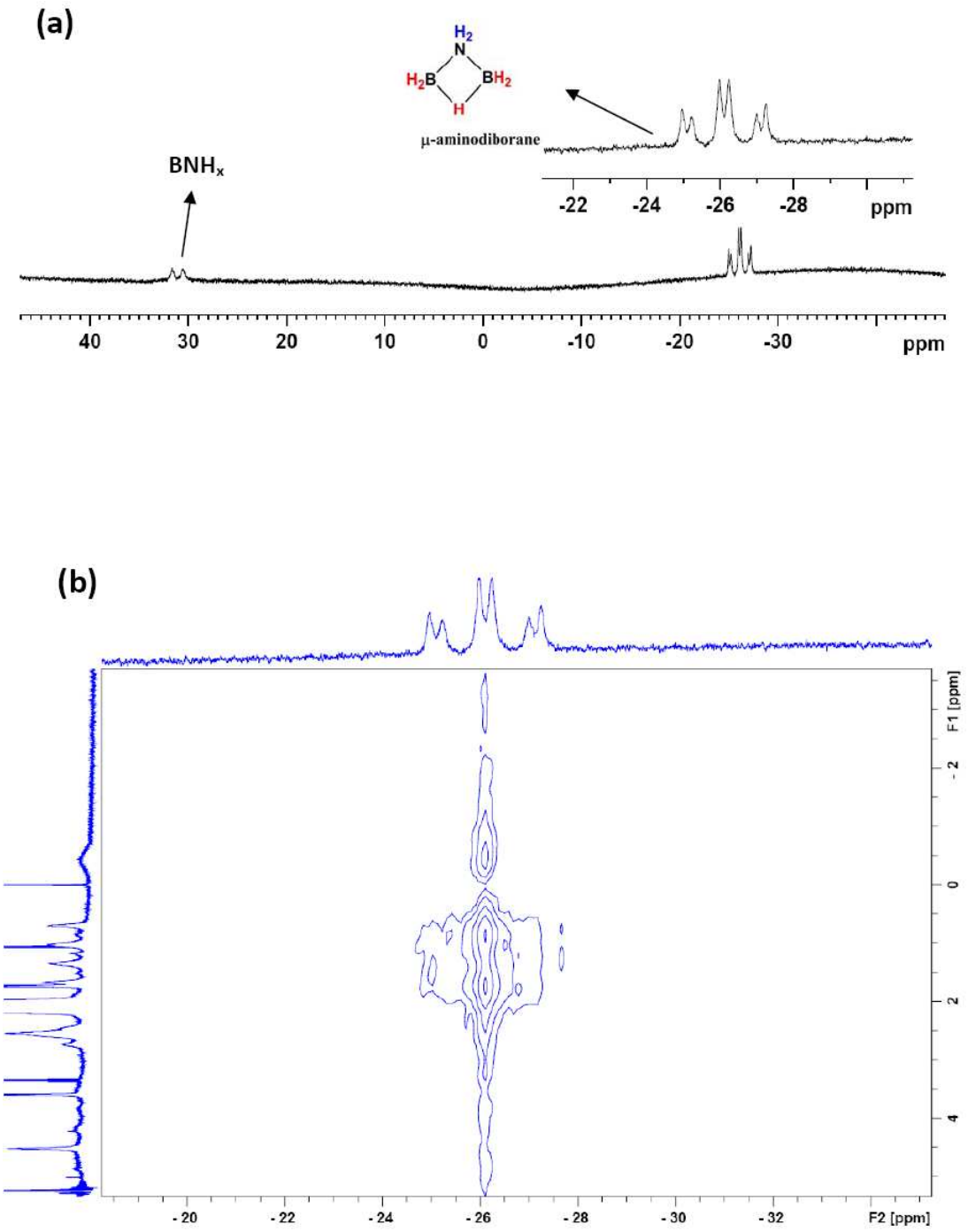

Figure S4. (a) ^{11}B NMR, (b) ^{1}H-^{11}B HETCOR spectral plot for the characterization of μ-aminodiborane

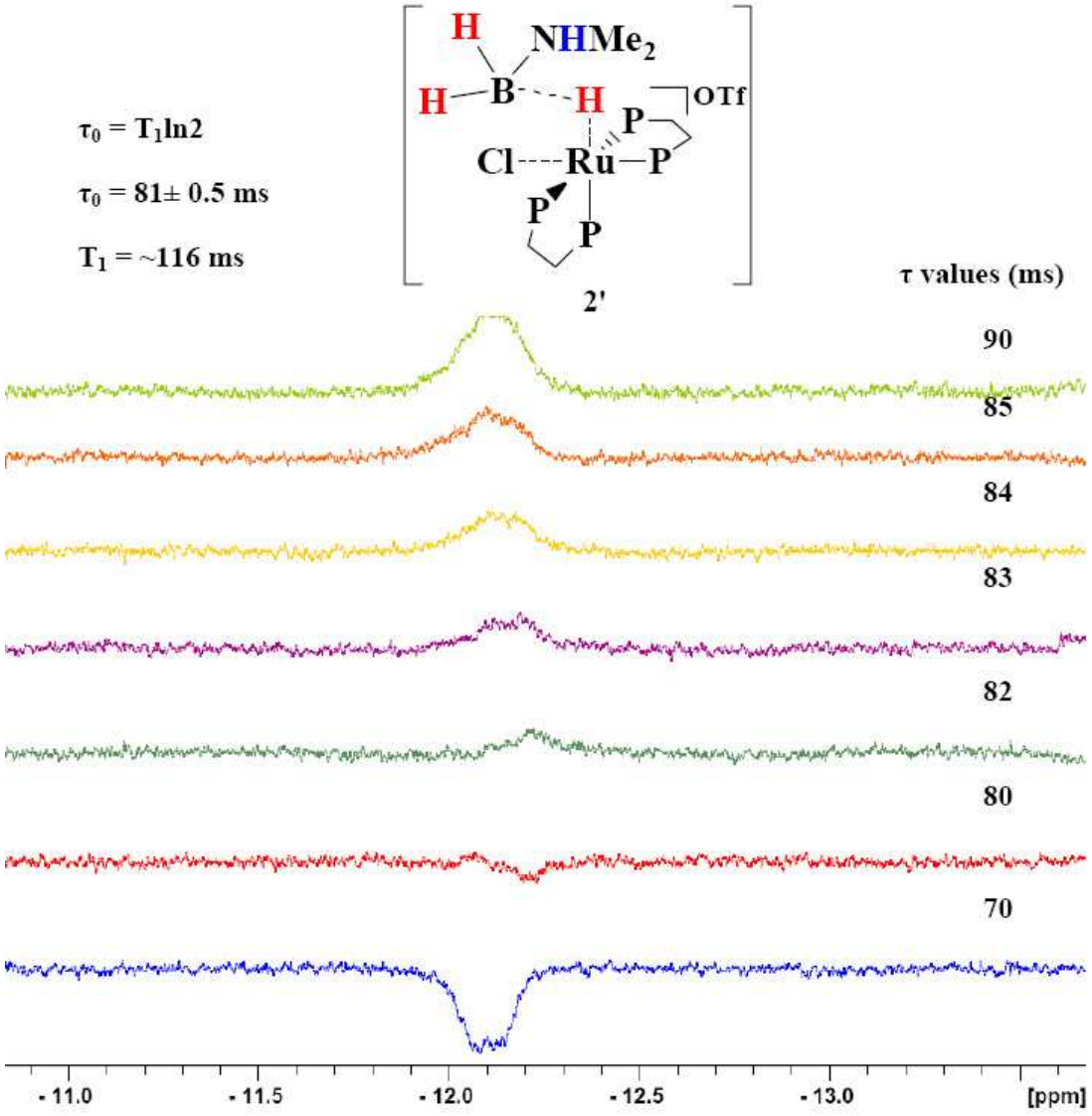

Figure S5. T_1 measurement of σ-borane intermediate (**2'**) at 193 K

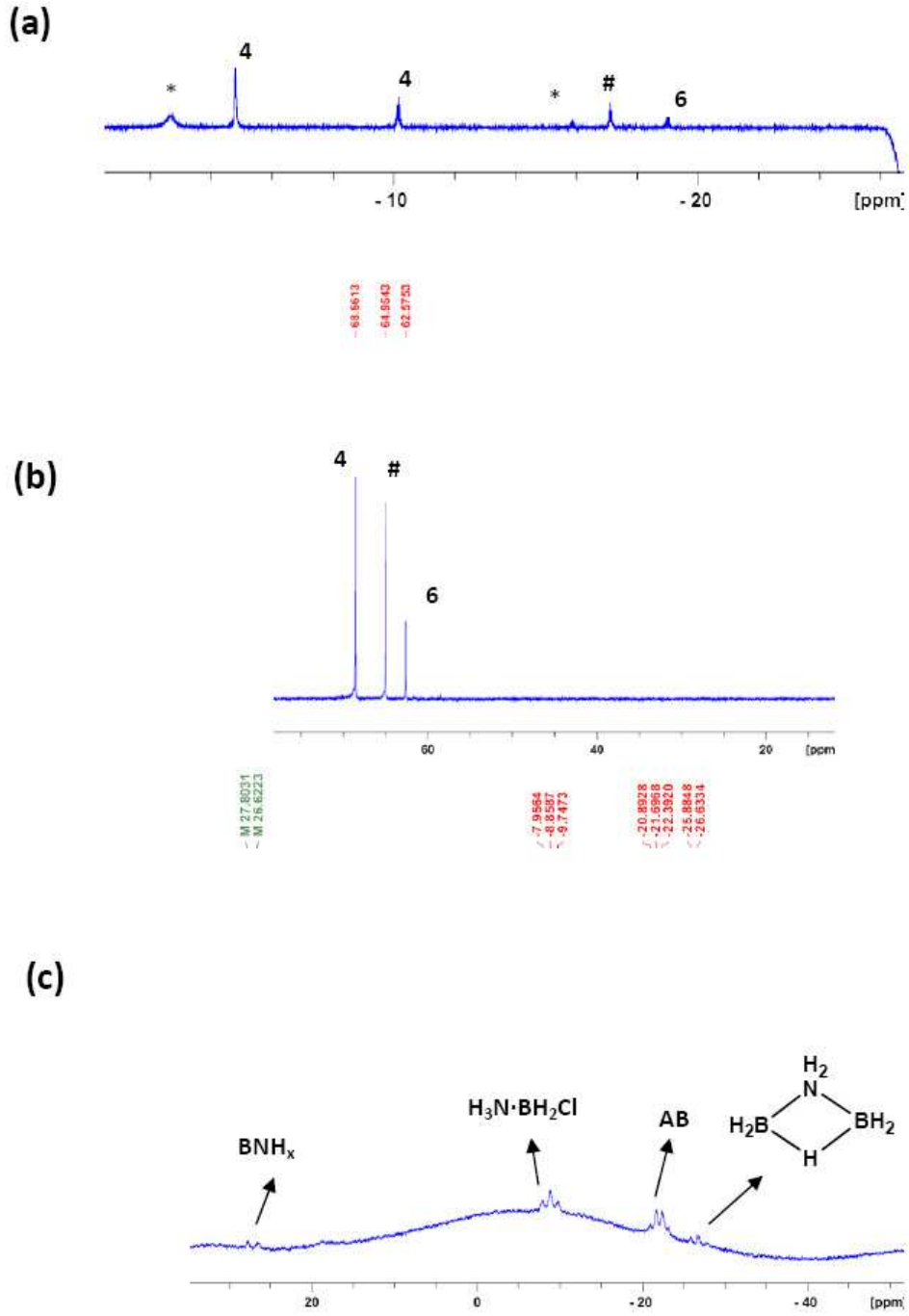

Figure S6. (a) ^{1}H, (b) $^{31}P\{^{1}H\}$, (c) ^{11}B NMR spectra of the reaction of complex **1** with excess AB at room temperature, # = $[Ru(H)(NH_3)(dppe)_2][OTf]$ * = unidentified

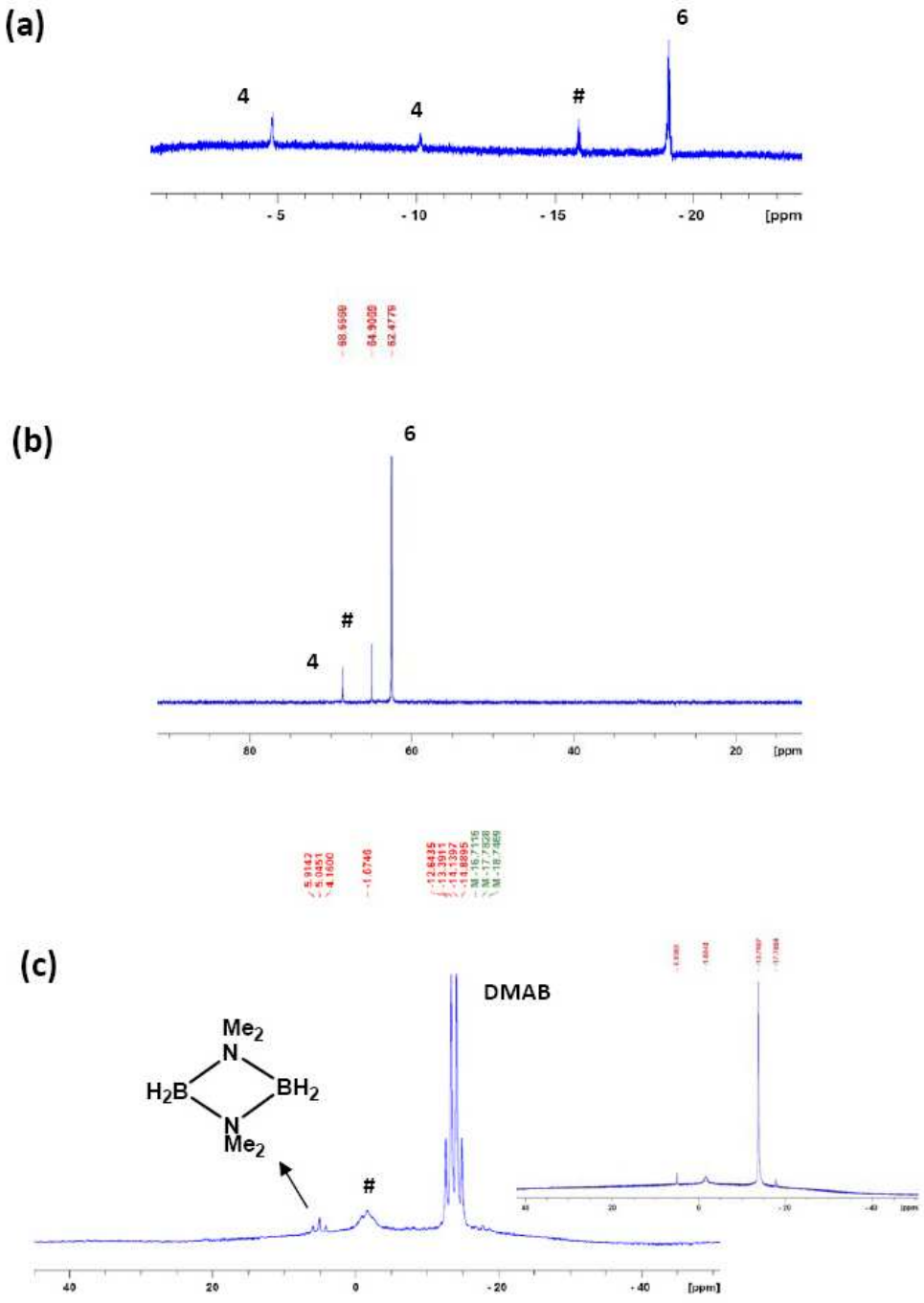

Figure S7. (a) ^{1}H, (b) $^{31}P\{^{1}H\}$, (c) ^{11}B NMR spectra of the reaction of complex **1** with excess DMAB at room temperature. # = unidentified

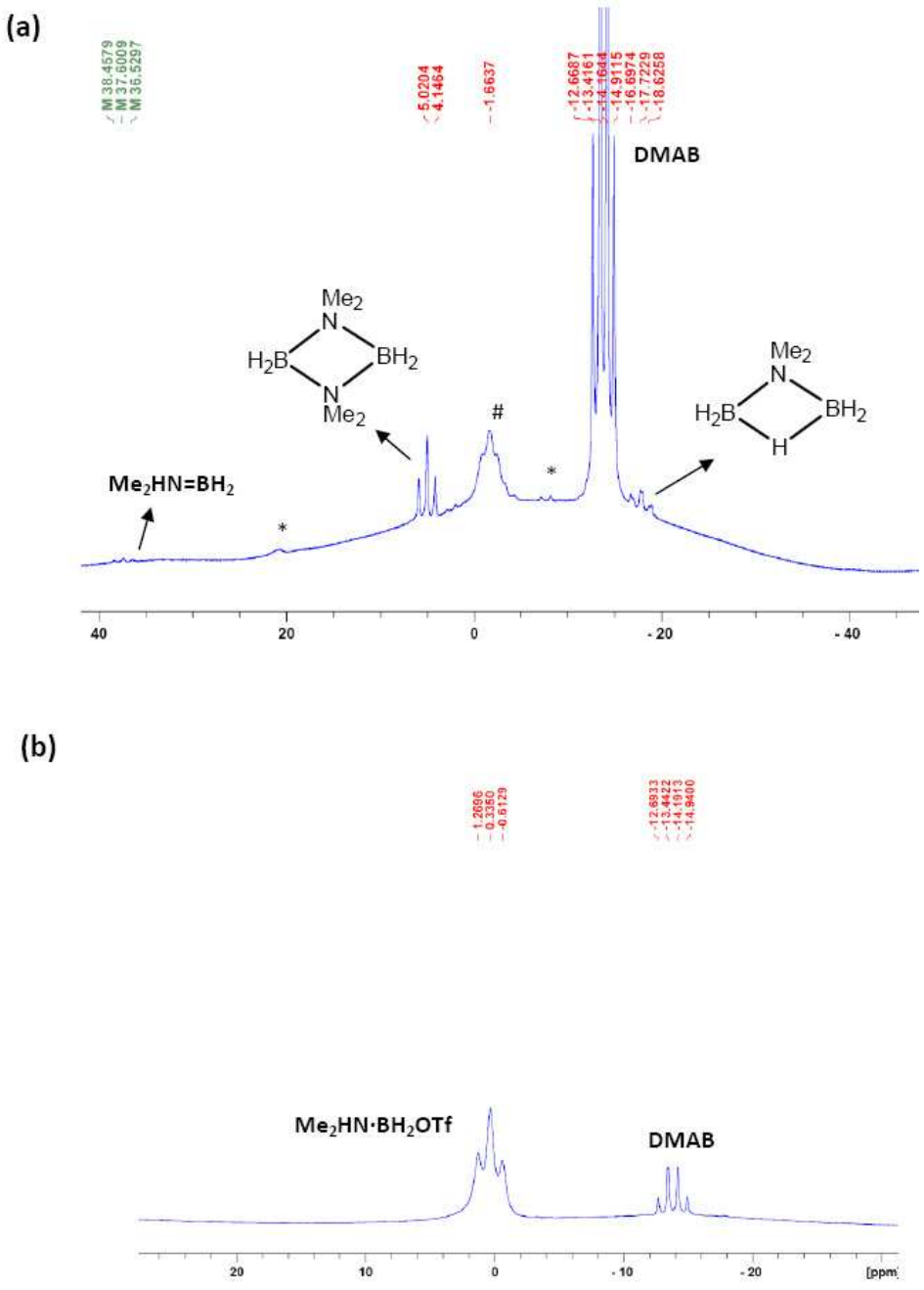

Figure S8. (a) ^{11}B NMR spectrum after long acquisition for the reaction of complex **1** with excess DMAB at room temperature, (b) reaction of HOTf and DMAB (1:1) showing $Me_2HN{\cdot}BH_2(OTf)$ (# = might be $(MeHN)_2BH_2$, * = not assigned yet)

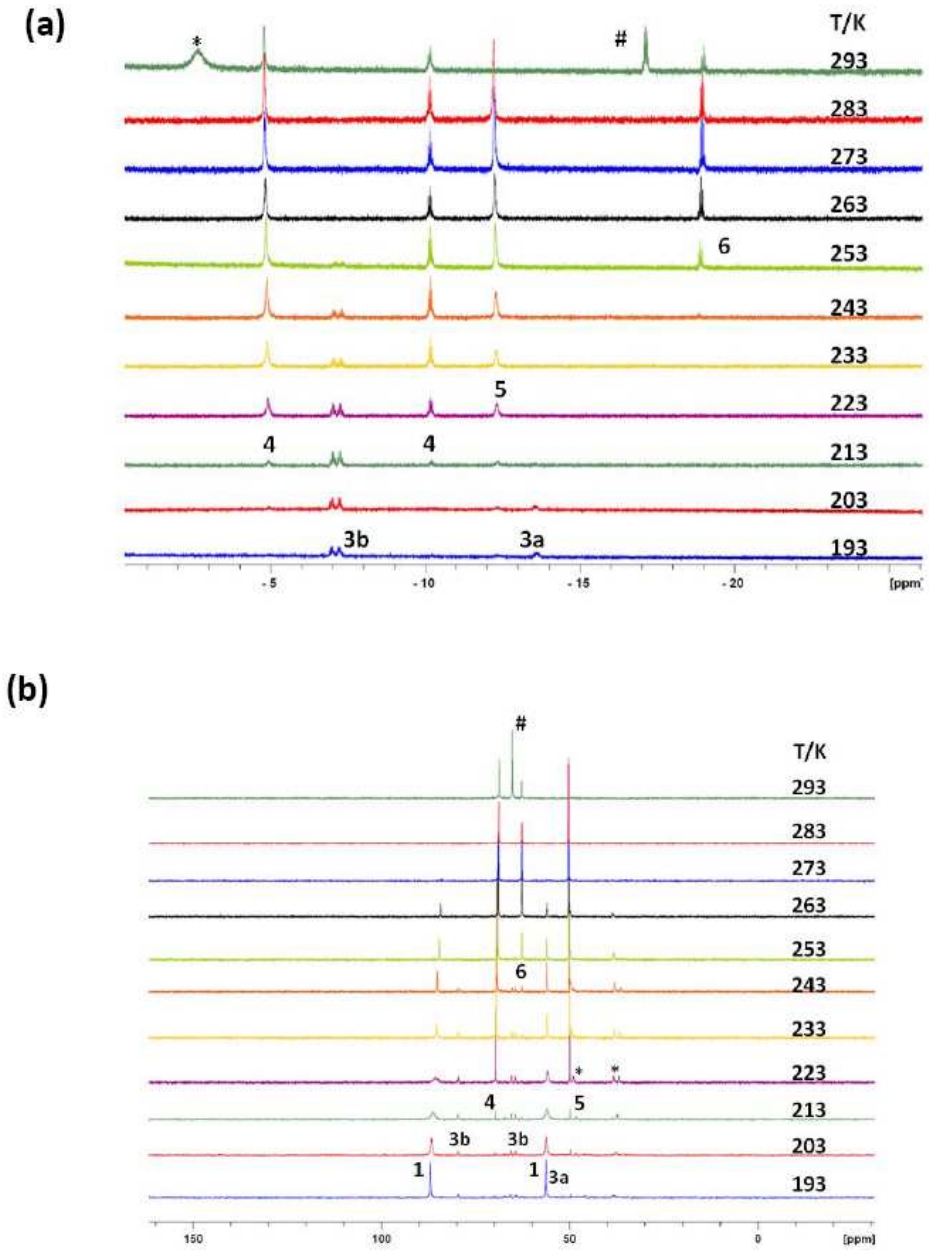

Figure S9. Variable temperature NMR spectral stack plots of (a) ^{1}H, (b) $^{31}P\{^{1}H\}$ NMR for the reaction of complex **1** with excess AB, # = $[Ru(H)(NH_3)(dppe)_2][OTf]$, * = *cis*-$[RuCl_2(dppe)_2]$

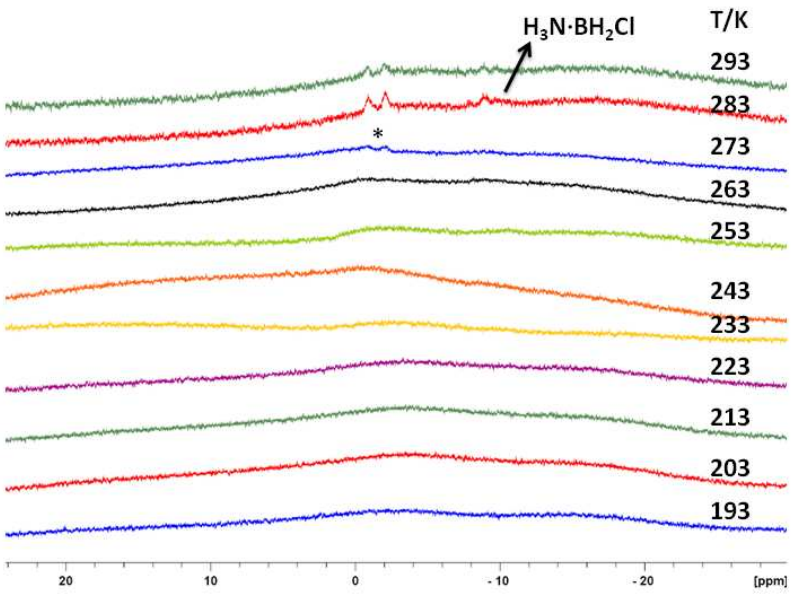

Figure S10. Variable temperature ^{11}B NMR spectral stack plots for the reaction of complex **1** with excess AB showing a very weak signal for $H_3N{\cdot}BH_2Cl$ and an unknown doublet (*) which may be $H_3N{\cdot}BHCl_2$

(a)

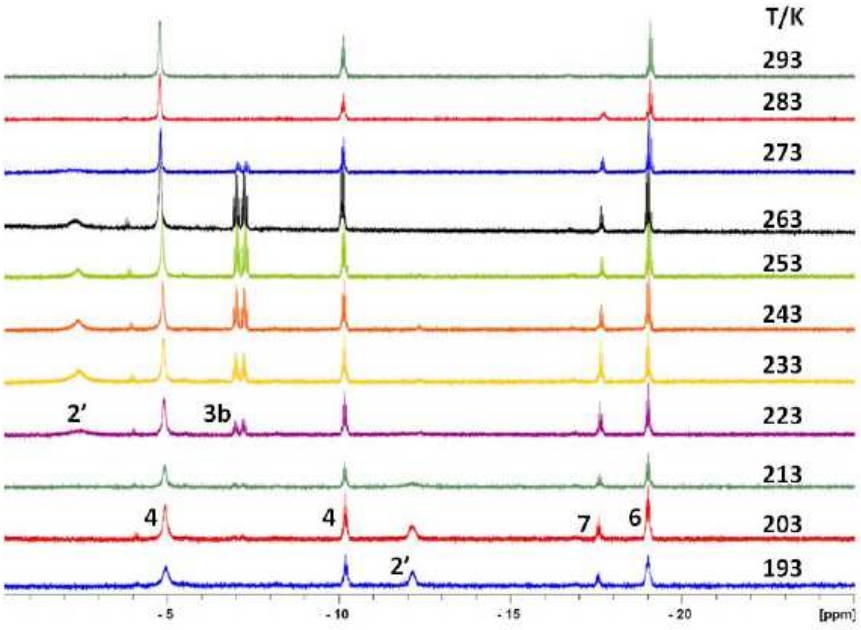

(b)

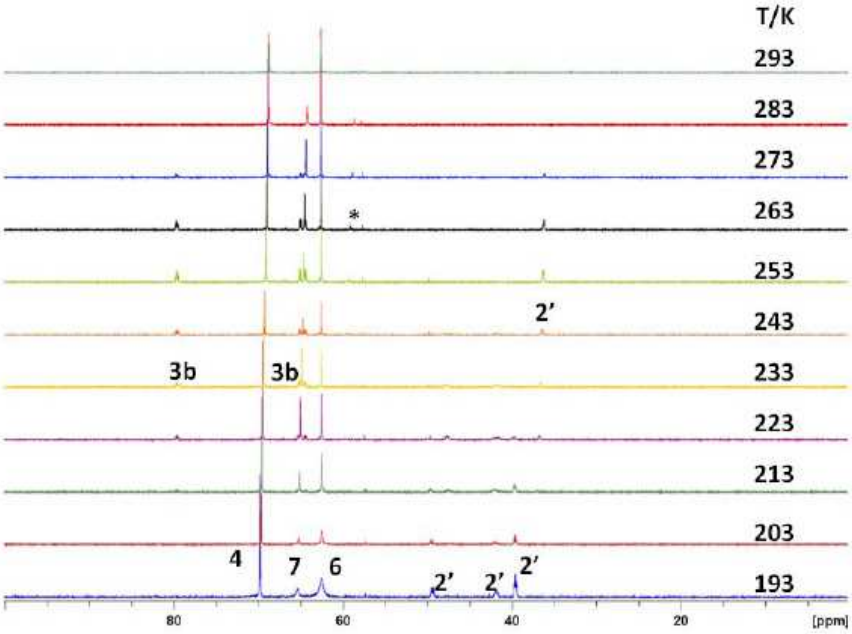

Figure S11. Variable temperature NMR spectral stack plots of (a) ^{1}H, (b) $^{31}P\{^{1}H\}$ NMR for the reaction of complex **1** with excess DMAB. * = unknown species.

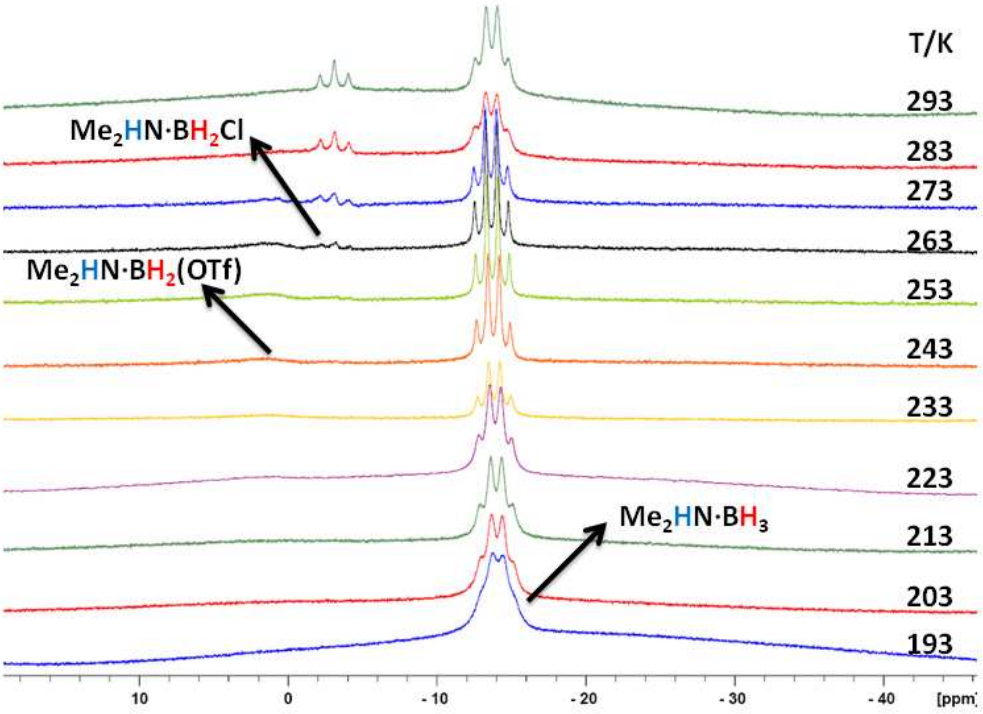

Figure S12. Variable temperature ^{11}B NMR spectral stack plots for the reaction of complex **1** with excess DMAB

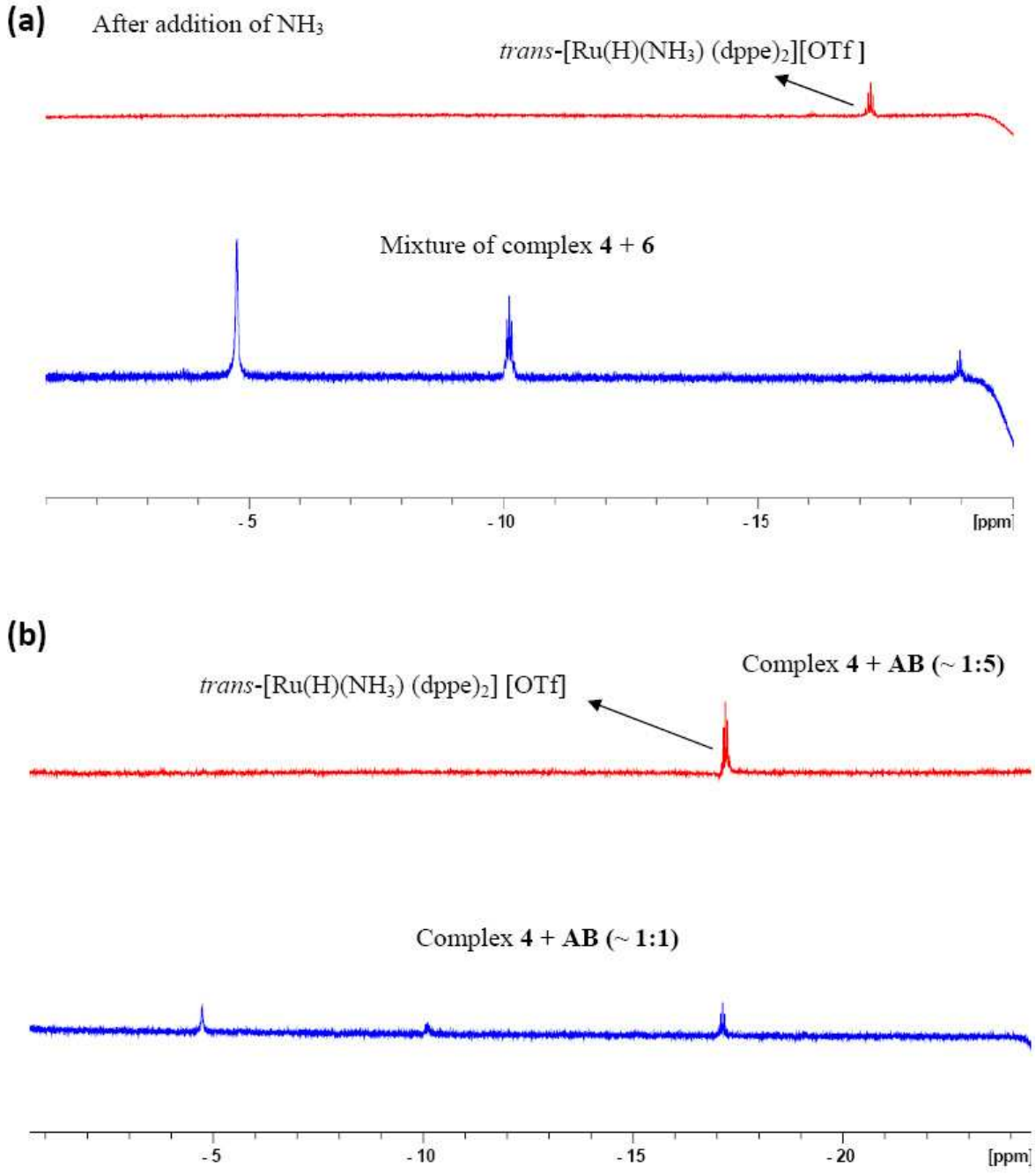

Figure S13. ^{1}H NMR spectral stack plot for the characterization of $[Ru(dppe)_2(H)(NH_3)][OTf]$: (a) addition of NH_3 to the reaction mixture of complex **4** and **6**, (b) reaction of AB with complex **4**

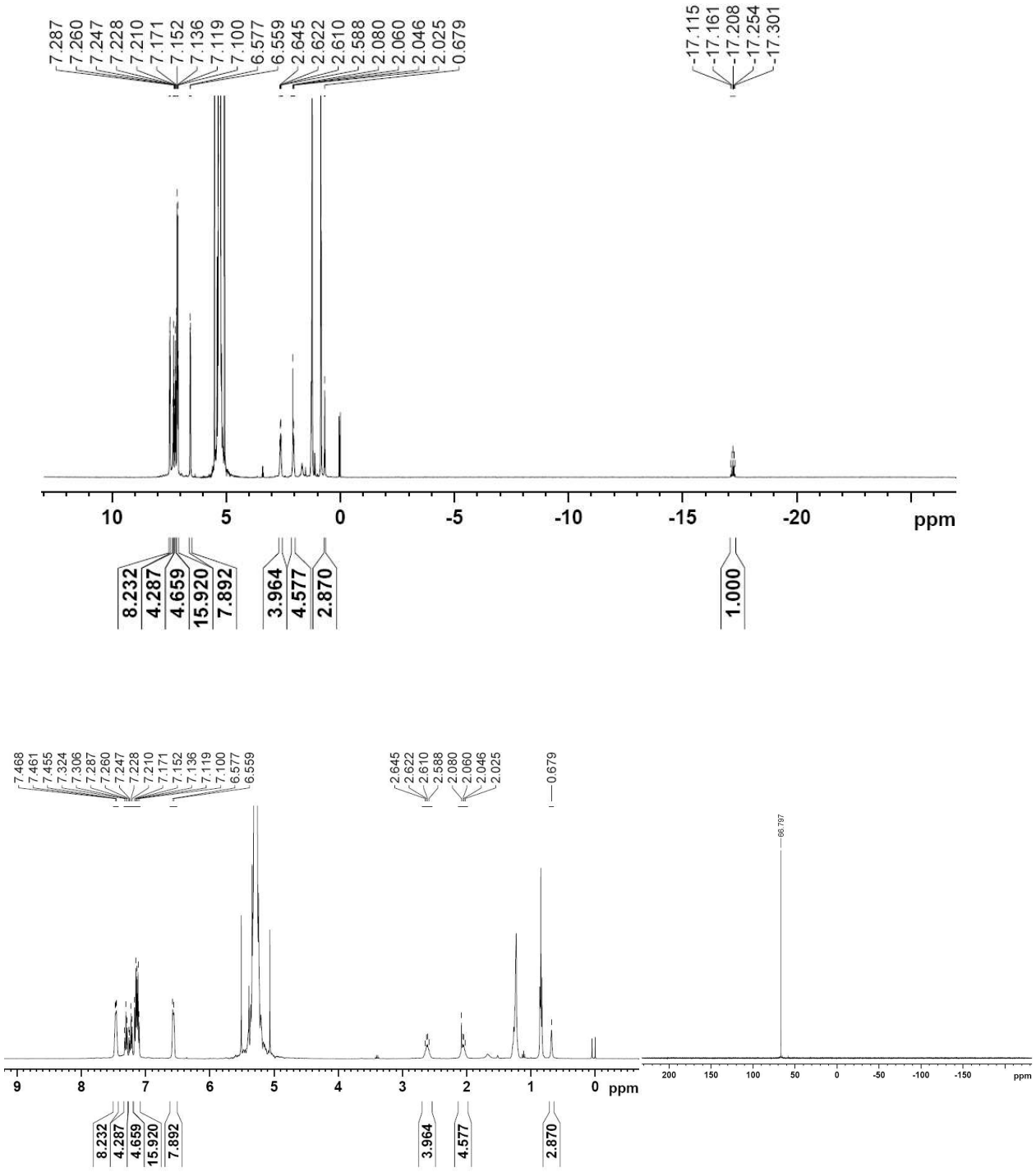

Figure S14. (a) ^{1}H, (b) $^{31}P\{^{1}H\}$ NMR spectra of $[Ru(dppe)_2(H)(NH_3)][OTf]$

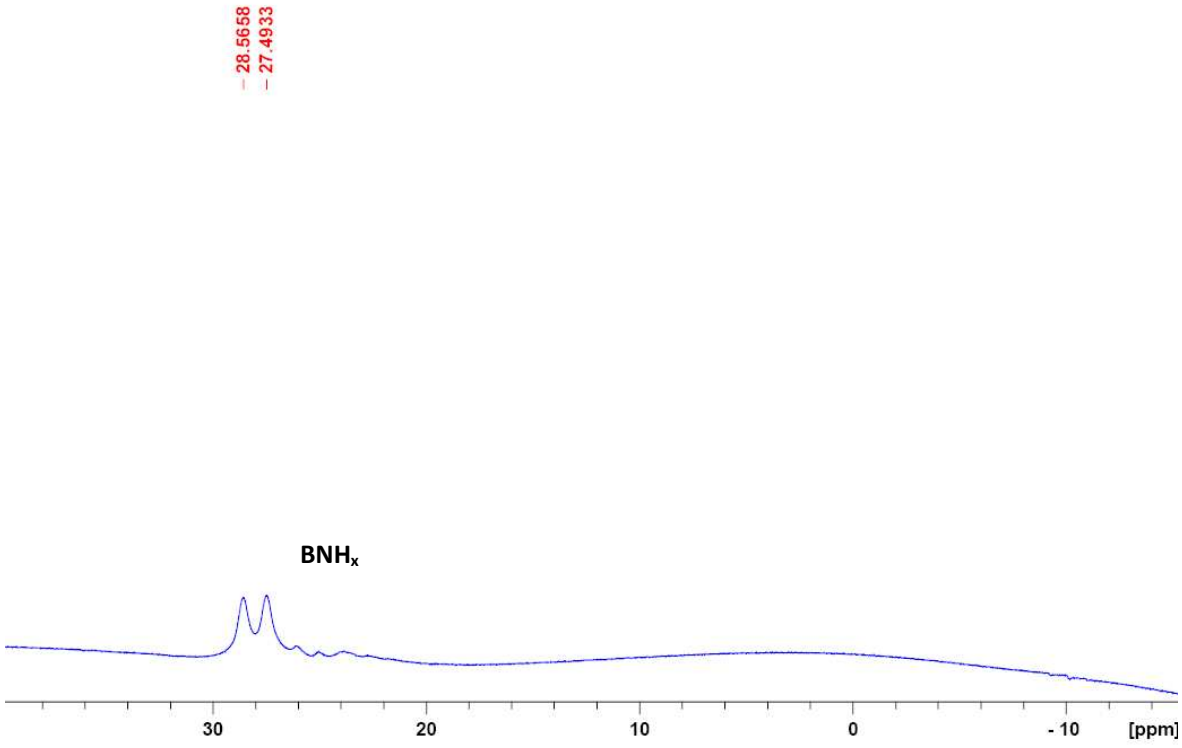

Figure S15. ^{11}B NMR spectra of off-white precipitate showing BNHx polymer

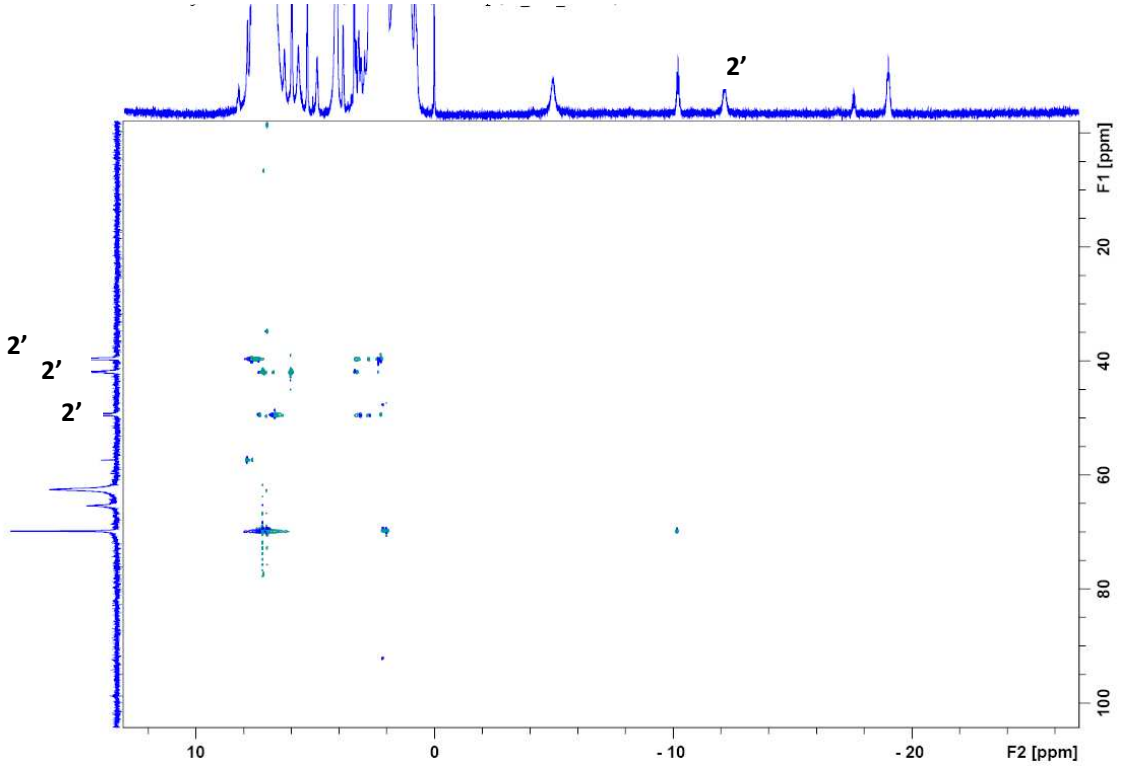

Figure S16. ^{1}H-^{31}P correlation spectrum showing no correlation spot for the intermediate **2'** even after 7 h of acquisition

Table S1. ^{31}P T_1 measurement data with temperature for complex **1** alone in CD_2Cl_2

Temperature (K)	Spin-Lattice Relaxation Time (T_1, ms)	
	P_{ax}	P_{eq}
193	361	188
213	318	173
233	433	173
253	563	267
273	592	354
293	707	505

Table S2. ^{31}P T_1 measurement data with temperature for complex **1** with AB in CD_2Cl_2

Temperature (K)	Spin-Lattice Relaxation Time (T_1, ms) for complexes				
	1		**4**	**5**	**6**
	[P_{ax}	P_{eq}]			
193	432	223	-[a]	-[a]	-[a]
203	403	187	-	-	-
213	389	194	-	-	-
223	446	223	-	-	-
233	518	230	432	-	317-360[b]
243	598	266	526	-	360-518
253	648	302	526-576[b]	-	374-432
263	677	331	461	691	418
273	792	346	518	864	490
283	-[a]	-[a]	634-677	1008	576
293	-	-	634-677	-[a]	634-648

Table S3. ^{31}P T_1 measurement data with temperature for complex **1** with DMAB in CD_2Cl_2

Temperature (K)	Spin-Lattice Relaxation Time (T_1, ms) for complexes				
	2'	**4**		**6**	**7**
		[Ru(η^2-H_2)	Ru-*H*]		
193	65	14-42[c]	-[a]	-[a]	216
203	72	14-42	-	-	230
213	86	14-42	-	-	245
223	58	14-42	-	-	245
233	58	14-42	-	259	230
243	86	14-42	288	274	230
253	274	14-42	302	288	245
263	259	14-42	317	302	245
273	230	14-42	346	317	274
283	-[a]	14-42	331	338	288
293	-	14-42	346	360	288-403[b]

Table S4. ^{1}H T_1 measurement data with temperature for complex **1** with DMAB in CD_2Cl_2

Temperature (K)	Spin-Lattice Relaxation Time (T_1, ms) for complexes					
	2'			**4**	**6**	**7**
	[P_{ax}	P_{eq}	$P_{eq'}$]			
193	504	360	360	360	-[a]	288
203	468	324	324	360	-	288
213	504	360	360	360	-	288
223[d]	-	432[d]	-	360	288	324
233	-	504	-	432	360	360
243	-	576	-	504	396	432
253	-	828	-	792	684	720
263	-[a]	-[a]	-[a]	648	540	540
273	-	-	-	648	576	576
283	-	-	-	648	576	576
293	-	-	-	576	684	-[a]

(a) Complex has either not appeared yet or consumed in the reaction or the null point was not observed in a defined range; (b) complex showed the null points in the range; (c) probable range of T_1 was observed; (d) **2'** undergoes rearrangement

Note: VT T_1 measurements were carried out using the inversion recovery method and the determination of a precise null point for each peak in the reaction mixture at every temperature was found to be rather difficult. There could be a maximum error up to ±25 in certain cases of ^{31}P T_1 data; in case of ^{1}H T_1 the error could be up to ±10 in some cases.

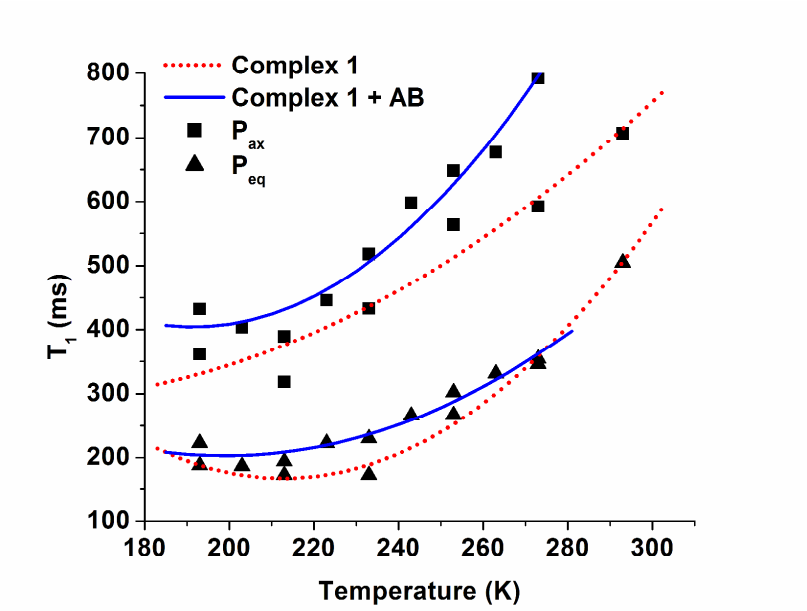

Figure S17. ^{31}P T_1 measurements plot with temperature for complex **1** alone (red-dotted line) and complex **1** with AB (blue smooth line) in CD_2Cl_2

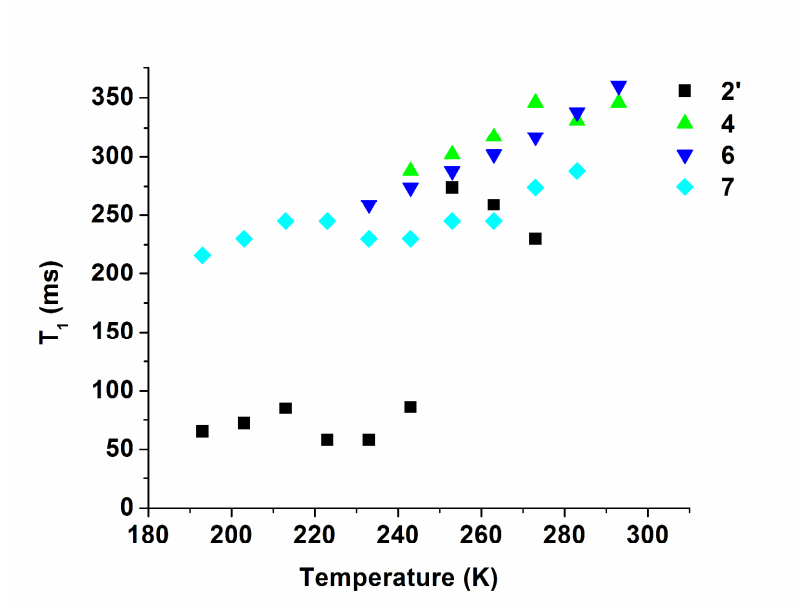

Figure S18. ^{1}H T_1 measurements plot with temperature for complex **1** with DMAB in CD_2Cl_2

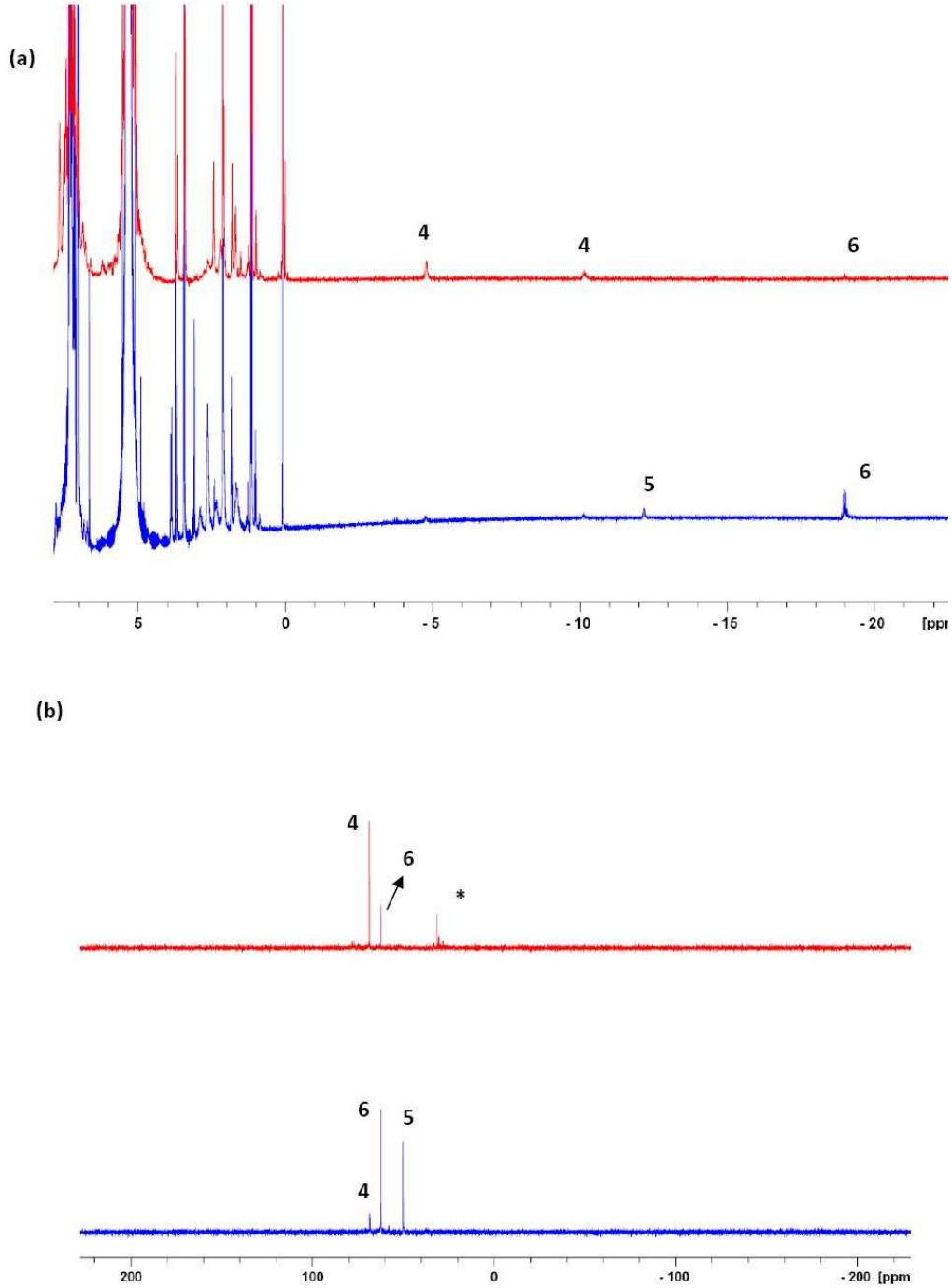

Figure S19. Conversion of **5** and **6** into **4**: (a) ^{1}H NMR spectral stack plot, (b) ^{31}P{^{1}H} NMR spectral stack plot with time (blue ~0 h, red ~12 h) * = decomposition products

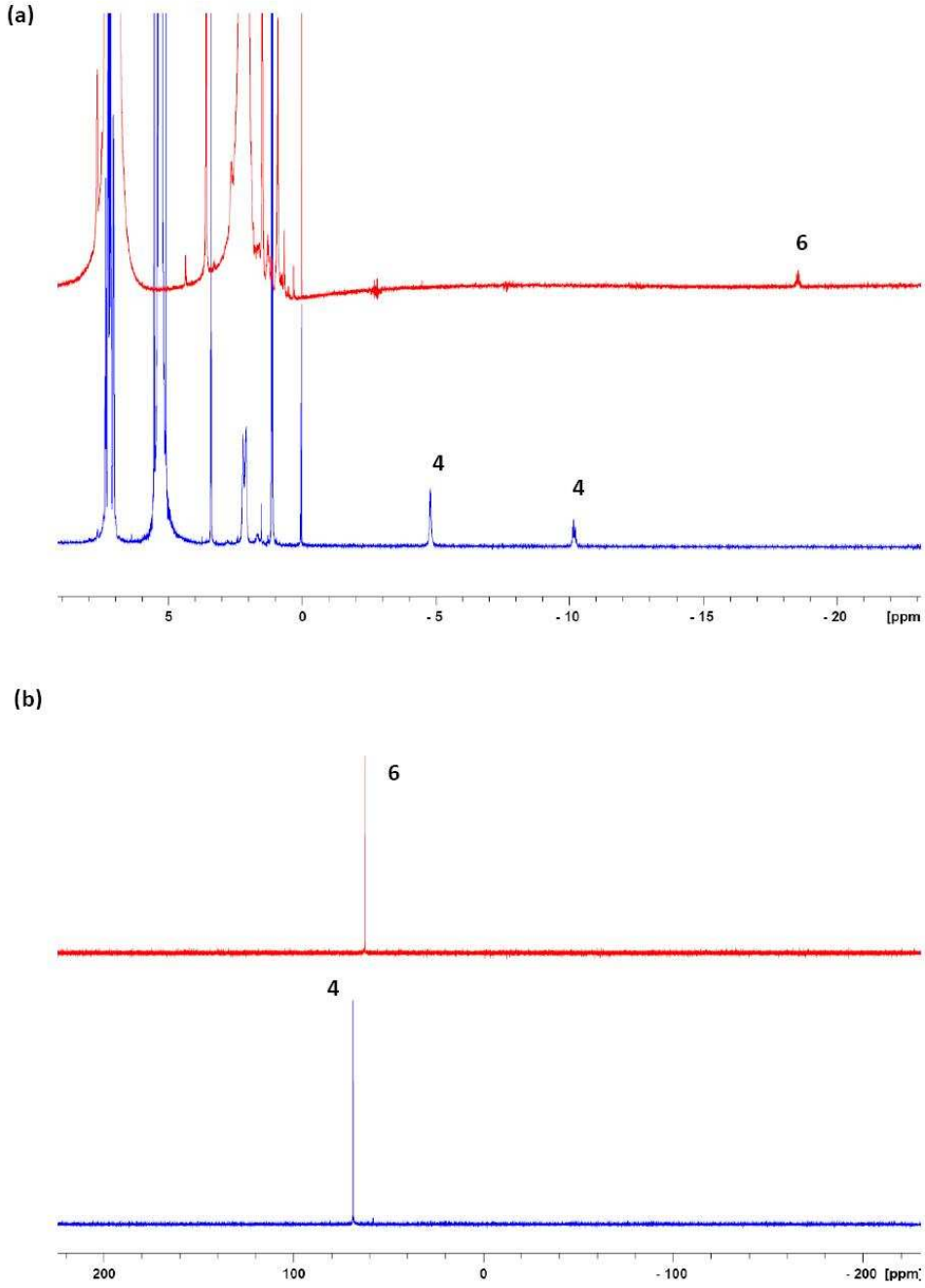

Figure S20. Conversion of **4** into **6**: (a) ^{1}H NMR spectral stack plot, (b) ^{31}P{^{1}H} NMR spectral stack plot after isolation of **4** and **6**. (stack plots are just for comparison)

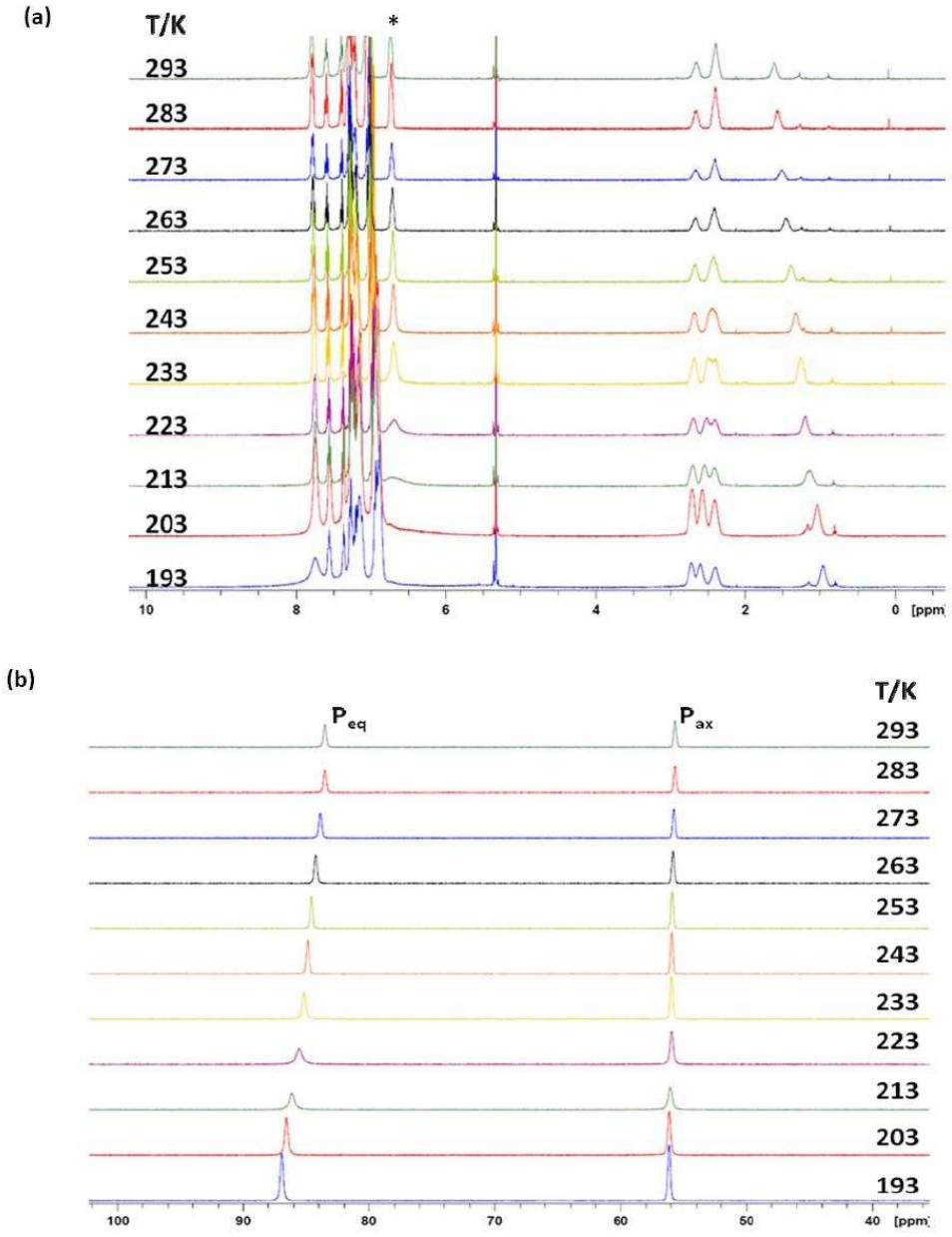

Figure S21. Variable temperature NMR stack plots for complex **1** (BLANK) in CD_2Cl_2: (a) ^1H NMR showing one of the phenyl region peak (*) getting broadened at low temperature; (b) ^{31}P NMR spectral stack plot showing the P_{ax} and P_{eq} signals getting broadened and resharpen with downfield shift at low temperature

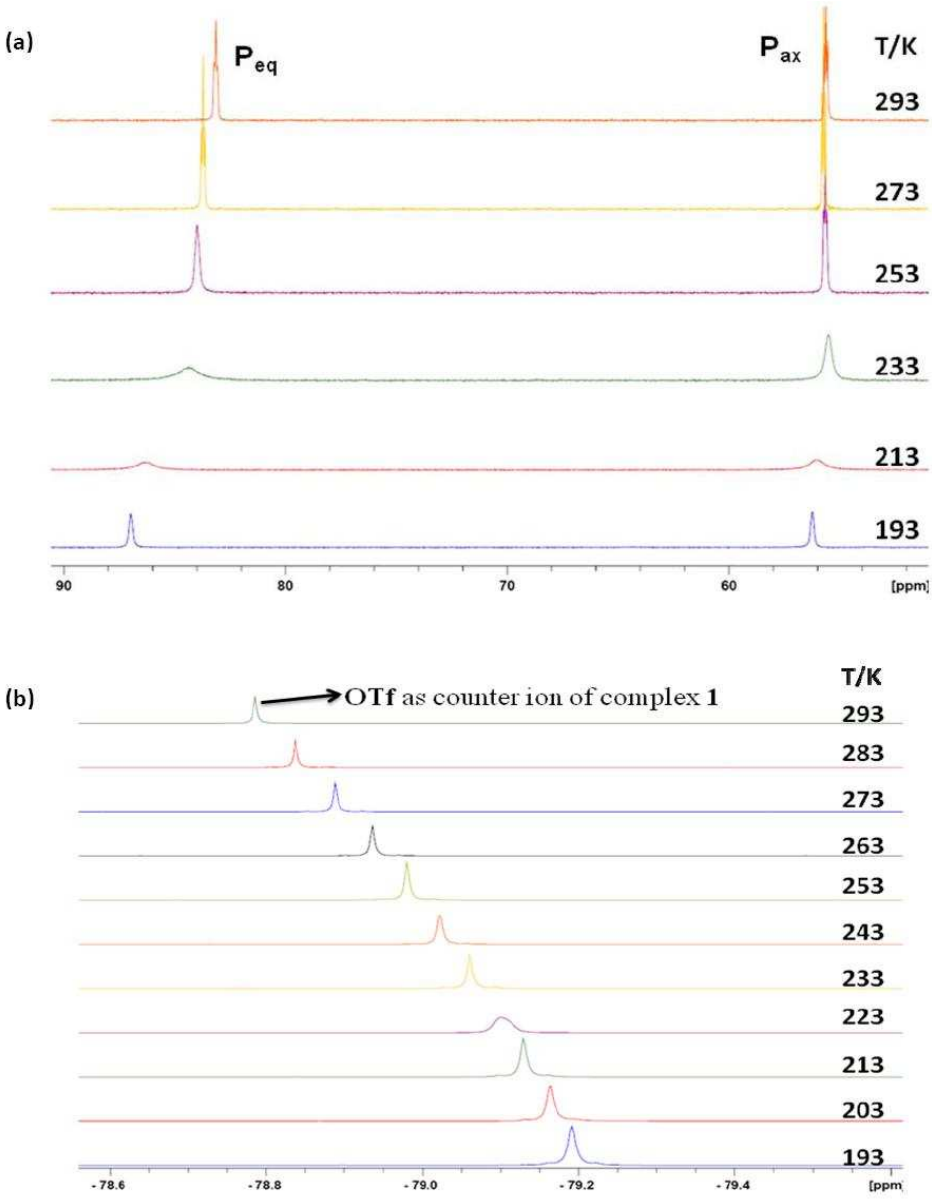

Figure S22. Variable temperature NMR spectral stack plots for complex **1** (BLANK) in CD_2Cl_2: (a) $^{31}P\{^1H\}$ NMR spectral stack plot showing the P_{ax} and P_{eq} signals getting broadened and resharpen with downfield shift at low temperature; (b)^{19}F NMR spectral stack plot showing a singlet for triflate (OTf) counter ion which broadened at 223 K and shifts upfield

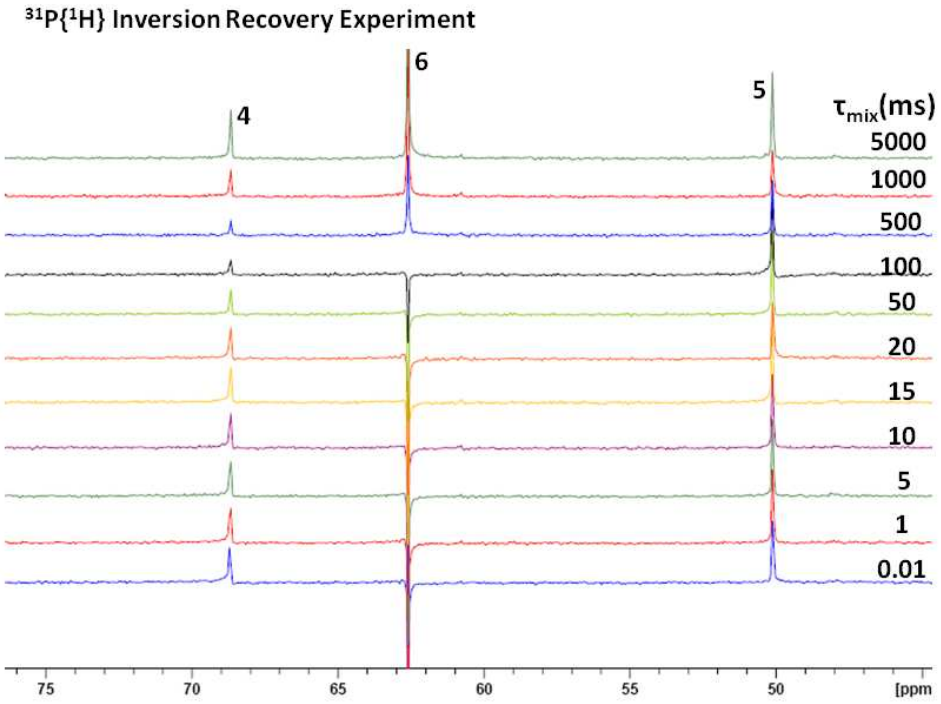

Figure S23. $^{31}P\{^{1}H\}$ Inversion recovery spectral stack plot for the reaction of complex **1** with DMAB in CD_2Cl_2 with mixing time delay (τ_{mix}) at room temperature showing change in intensity of **4** when **6** is inverted selectively and recovered with τ_{mix}

(a)

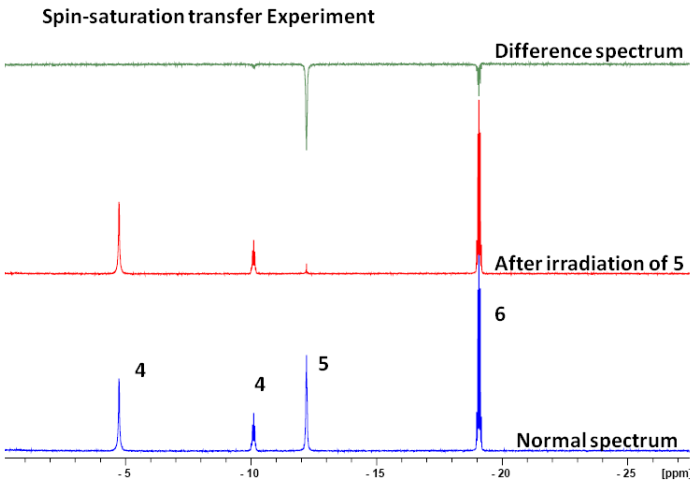

(b)

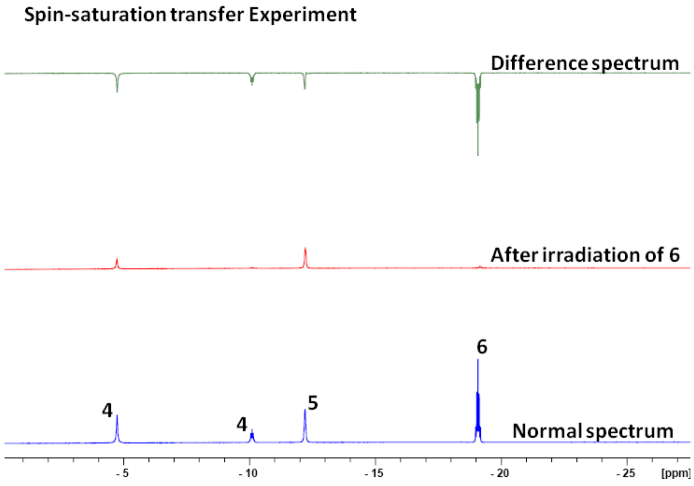

Figure S24. Spin-saturation transfer experiment: ^{1}H NMR (upfield region) spectral stack plots for the reaction of complex **1** with DMAB in CD_2Cl_2 at room temperature; (a) irradiation of **5**, (b) irradiation of **6**

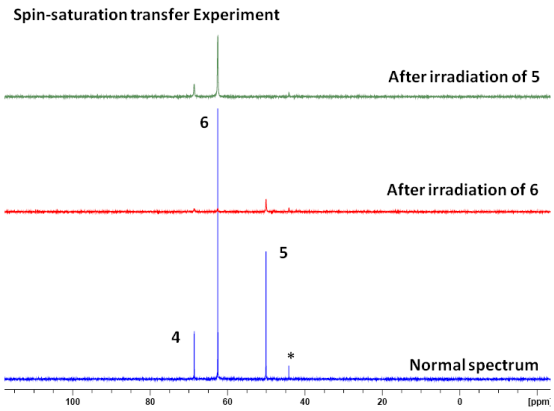

Figure S25. $^{31}P\{^{1}H\}$ Spin-saturation transfer spectral stack plot for the reaction of complex **1** with DMAB in CD_2Cl_2 at room temperature,* = *trans*-[$RuCl_2(dppe)_2$]

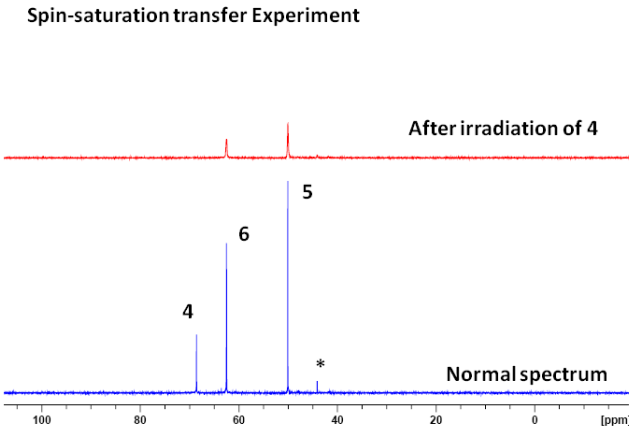

Figure S26. $^{31}P\{^{1}H\}$ Spin-saturation transfer spectral stack plot for the reaction of complex **1** with DMAB in CD_2Cl_2 at room temperature after irradiation of **4**, * = *trans*-[$RuCl_2(dppe)_2$] (Note: spectra in Figures S25 and S26 are from different batches)

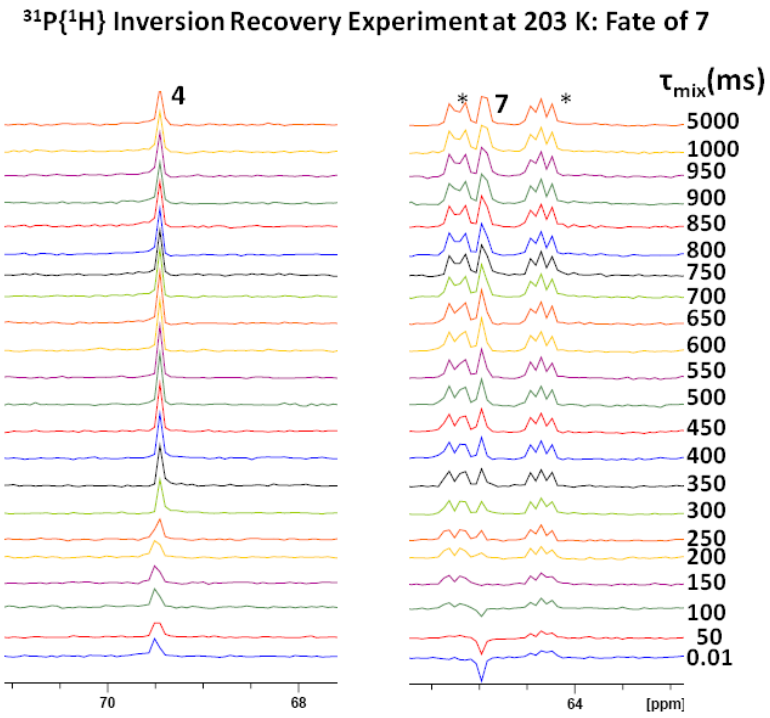

Figure S27. $^{31}P\{^{1}H\}$ Inversion recovery spectral stack plot for the reaction of complex **1** with DMAB in CD_2Cl_2 with mixing time delay (τ_{mix}) at 203 K showing change in intensity of **4** when **7** is inverted selectively and recovered with τ_{mix}, * = **3b** is also getting affected. **Note**: only the peaks getting affected after inversion of **7** and during its recovery are shown